

NASA-CR-193828

169215  
p. 39



SHUTTLE PRCS  
PLUME CONTAMINATION ANALYSIS  
FOR ASTRO-2 MISSION  
(5-33173)

April 1993

Final Technical Report for the Period  
February 24, 1993 through April 30, 1993

(NASA-CR-193 828 SHUTTLE PRCS  
PLUME CONTAMINATION ANALYSIS FOR  
ASTRO-2 MISSION Final Technical  
Report, 24 Feb. - 30 Apr. 1993  
(Alabama Univ.) 39 p

N93-27240

Unclas

G3/20 0167275

**Research Institute  
The University of Alabama in Huntsville**

Technical Report No. 5-33173  
Contract Number FNAS WANG MSFC PO  
Purchase Order No. P.O. H-18069D

**SHUTTLE PRCS  
PLUME CONTAMINATION ANALYSIS  
FOR ASTRO-2 MISSION  
(5-33173)**

April 1993

Final Technical Report for the Period  
February 24, 1993 through April 30, 1993

Prepared by:

Dr. F. C. Wang  
C. Greene

Research Institute  
The University of Alabama in Huntsville  
Huntsville, Alabama 35899

Prepared for:

NASA George C. Marshall Space Flight Center  
Marshall Space Flight Center, AL 32512

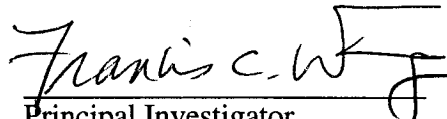
Attn: Miria Finckenor  
Materials and Processes Laboratory  
EH12

## Preface

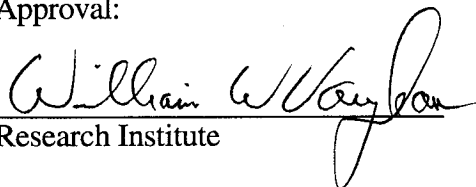
This technical report was prepared by the staff of the Research Institute, The University of Alabama in Huntsville. It documents the research performed under Delivery Order P.O. H-18069D. Dr. Francis C. Wang was the Principal Investigator. Technical work was accomplished by Dr. Wang, supported by Ms. Cindy Greene. This work was performed in cooperation with the Engineering Physics Division of the Materials and Processes Laboratory and the Thermal Control Engineering Branch of the Structure and Dynamics Laboratory at the Marshall Space Flight Center. Ms. Miria Finckenor of MSFC Materials and Processes Laboratory, EH12, was the COTR and provided technical coordination and input. Mr. David Jacobson of MSFC Astro Chief Engineers Office provided funding support.

The views, opinions, and/or findings contained in this report are those of the author(s) and should not be construed as an official National Aeronautics and Space Administration, Marshall Space Flight Center position, policy, or decision unless so designated by other official documentation.

I have reviewed this report, dated 30 April 1993, and the report contains no classified information.

  
Principal Investigator

Approval:

  
Research Institute

## **Acknowledgment**

The authors gratefully acknowledge the assistance they have received from the following individuals during the course of this study: Mr. Larry French of Teledyne Brown Engineering for providing technical information related to Astro instruments and mission; Mr. Basil Cooper of Boeing Aerospace Company for assistance in the execution of the MOLFLUX code; Mr. S. D. Smith of SECA, Inc, for discussion on plume modeling; Ms. Sheryl Kittredge of MSFC for generating the view factors and using TRASYS code.

Special thanks go to Ms. Miria Finckenor of MSFC for her effort in conducting MOLFLUX code runs and providing various assistance during the course of this study.

## Abstract

The Astro-2 mission scheduled for January 1995 flight is co-manifested with the Spartan experiment. The Astro instrument array consists of several telescopes operating in the UV spectrum. To obtain the desired 300 observations with the telescope array in a shorter time than the Astro-1 mission, it will be necessary to use the primary reaction control system (PRCS) rather than just the Vernier reaction control system. The high mass flow rate of the PRCS engines cause considerable concern about contamination due to PRCS plume return flux.

Performance of these instruments depends heavily on the environment they encounter. The ability of the optical system to detect a remote signal depends not only on the intensity of the incoming signal, but also on the ensuing transmission loss through the optical train of the instrument. Performance of these instruments is thus dependent on the properties of the optical surface and the medium through which it propagates. The on-orbit contamination environment will have a strong influence on the performance of these instruments.

This report summarizes the finding of a two-month study of the molecular contamination environment of the Astro-2 instruments due to PRCS thruster plumes during the planned Astro-2 mission.

## Acronyms

AO	Atomic Oxygen
AST	Astro Star Tracker
BKG	Bhatnagar-Gross-Krook
CONTAM	Plume Contamination Effects Prediction
COTR	Contracting Office's Technical Representative
DSMC	Direct Simulation Monte Carlo
FOV	Field of View
HUT	Hopkins Ultraviolet Telescope
IPS	Instrument Pivoting Structure
IR	Infrared
JSC	Johnson Space Center
LEO	Low Earth Orbit
LOS	Line of Sight
MAPTIS	Material and Processes Technical Information System
MMH	Mono-Methyl Hydrazine
MOC	Method of Characteristics
MOLESCAT	Molecular Scattering Program
MOLFLUX	Molecular Flux Program
MSFC	Marshall Space Flight Center
NASA	National Aeronautics and Space Administration
OMS	Orbital Manuvering System
OSP	Optical Sensor Package
PRCS	Primary Reaction Control System
PSSA	Payload Support Strut Assembly
RCS	Reaction Control System
RAMP	Reacting and Multi-phase Program
SPACE	Shuttle/Payload Contamination Evaluation
SPIE	Shuttle Plume Impingement Experiment
STS	Space Transportation System
TRASYS	Thermal Radiation Analysis System
UAH	University of Alabama in Huntsville
UIT	Ultraviolet Imaging Telescope
UV	Ultraviolet
VOFMOC	Variable Oxidizer/Fuel Ratio Method of Characteristics
VRCS	Vernier Reaction Control System
VUV	Vacuum Ultraviolet
WUPPE	Wisconsin Ultraviolet Photo-Polarimeter Experiment

## Table Of Contents

1.0	INTRODUCTION.....	1
1.1	Problem Definition.....	1
1.2	The Shuttle RCS System.....	1
1.3	Plume Contamination Concerns.....	2
2.0	ANALYTICAL APPROACH.....	3
2.1	Molecular Transport at LEO .....	3
2.2	Plume Flowfield Description .....	4
2.3	Contamination Analysis Tools.....	4
2.4	Operations of the MOLFLUX Code .....	5
3.0	RESULTS AND DISCUSSION.....	6
3.1	PRCS Return Flux.....	6
3.2	Column Density Results.....	6
3.3	Effects of Deposition on Instruments.....	7
4.0	LESSONS LEARNED AND RECOMMENDATIONS.....	9
4.1	Lessons Learned in MOLFLUX Operations.....	9
4.2	Recommendation for Future Studies.....	9
	REFERENCES .....	11

## List Of Figures

1.1	Astro-2 Payload Configuration.....	13
1.2	Shuttle Orbiter Configuration and Coordinates.....	14
1.3	RCS Thruster Identification .....	15
1.4	Plume Contamination Damage .....	16
1.5	Effects of MMH-HNO <sub>3</sub> Deposit on Selected Optical Surfaces.....	17
2.1	Typical Plume Flowfield Regions .....	18

## List Of Tables

1.1	Nominal Components and Application Locations for Shuttle RCS.....	19
1.2	Mole Fraction of Engine Exhaust.....	20
2.1	Gasdynamic & Contamination Analysis Tools.....	21
2.2	Input File Requirements.....	22
3.1	Self Scattering Return Flux, H <sub>2</sub> O.....	23
3.2	Self Scattering Return Flux, Unburned Fuel.....	23
3.3	Self Scattering Return Flux, Total.....	24
3.4	Ambient Scattering Return Flux, H <sub>2</sub> O.....	24
3.5	Ambient Scattering Return Flux, Unburned Fuel.....	25
3.6	Ambient Scattering Return Flux, Total.....	25
3.7	Ambient Scattering Return Flux, H <sub>2</sub> O.....	26
3.8	Ambient Scattering Return Flux, Unburned Fuel.....	26
3.9	Ambient Scattering Return Flux, Total.....	27
3.10	Column Density in +Z Direction (BGK Results).....	27
3.11	Maximum Column Density (BGK Results).....	28
3.12	Column Density, H <sub>2</sub> O.....	28
3.13	Column Density, CO <sub>2</sub> .....	29
3.14	Column Density, Total.....	29

## 1.0 INTRODUCTION

The performance of a space-borne optical system depends heavily on the surface properties, such as reflectivity and transmissivity, of its elements. These performance parameters could be adversely affected through the accumulation of surface contaminants. The detection of optical signals may also be affected by the existence of contaminants in the surrounding environment. Knowledge of the contamination environment is thus critical to ensure the long-term performance of space-borne observatories.

### 1.1 Problem Definition

The Astro-2 instruments considered in this study are the Hopkins Ultraviolet Telescope (HUT), the Wisconsin Ultraviolet Photo-Polarimeter Experiment (WUPPE), and the Ultraviolet Imaging Telescope (UIT). These instruments are mounted on an Instrument Pivoting Structure (IPS) which can pivot the whole assembly 90 degrees from its berthing position to the observation position. Also located on the IPS are an Astro Star Tracker (AST) and an Optical Sensor Package (OSP). During launch and earth return phases of the mission, the payload assembly is berthed to the Payload Support Strut Assembly (PSSA), while in the observation mode the instruments are pointing in the +Z direction out the Orbiter bay, as shown in Figure 1.1.

The Astro-2 mission is currently scheduled for January 1995 and is co-manifested with the Spartan experiment. To obtain the desired 300 some observations with the telescope array in a shorter time than the Astro-1 mission, it will be necessary to use the primary reaction control system (PRCS) rather than just the Vernier reaction control system (VRCS) for pointing control. Due to the high thrust level of the PRCS engines, there is considerable concern about contamination effects to the Astro-2 instruments.

### 1.2 The Shuttle RCS System

The Shuttle Orbiter has 6 VRCS and 38 PRCS engines for on-orbit maneuvering, such as orbit changes, and orientation adjustment, and for pointing control. The VRCS uses engines with a thrust of 24 pounds, and the PRCS uses engines with 870 pound thrust. Both engines use the mono-methyl hydrazine (MMH) bi-propellant. These engines are clustered in three groups as the forward RCS, the left hand RCS, and the right hand RCS, as shown in figure 1.2. The RCS thruster identification and relative locations are shown in Figure 1.3, and the nominal components and application of all RCS are listed in Table 1.1.

It has been determined that of all RCS thrusters, only the nine +Z firing PRCS will pose as contamination threats to the Astro-2 instrument array. Hence the analysis will be limited to plumes generated by the firing of these nine PRCS thrusters. The nine engines are identified as F1U, F2U, and F3U located in the nose of the Orbiter, and the L1U, L2U, and L4U, and the R1U, R2U, and R4U engines located at the aft end of the orbiter on the left and the right OMS pods, respectively.

### 1.3 Plume Contamination Concerns

The effects on space vehicle surfaces due to rocket exhaust products have been the subject of extensive investigation [1-5]. The overall damage mechanism can be summarized in Figure 1.4 as due to deposition of gaseous components and abrasion by high speed droplets or particulates. Based on laboratory studies using small bi-propellant engines, the distribution of droplets is found to be concentrated in the region near the axis of the plume. The damage mechanism in this region is then due to impingement by small fast-moving droplets causing abrasion and deposition damages. In the outer region away from the axis, most plume products are gaseous, and the damage mechanism in this region is due to condensation of unburned fuel vapor. At large angles, large slow moving droplets are generated from the liquid nozzle wall film. The deposition of these large droplets is the major contamination damage mechanism in this region.

Laboratory data indicates that the most commonly noted contaminants are water and the low volatility mixture of water, MMH, and salts such as methylhydrazinium nitrate[6]. However, most available laboratory experimental data on the effects of the combustion products on optical surfaces is in the infrared wavelength. Data on optical surface degradation in the UV wavelength is very limited. Liu and Glassford [1] conducted limited laboratory tests of liquid and solid MMH-HNO<sub>3</sub> deposited on several thermal control surfaces and on fused silica at 25°C. The data, presented in terms of spectral reflectance degradation in Figure 1.5, indicates that the solar absorptance of the thermal control surfaces measured *ex situ* generally increases with deposit mass; that MMH-HNO<sub>3</sub> absorbs strongly in the UV and visible wavelength ranges; and that the degradation of fused silica is greatest in the UV region and significant in the IR region at large deposit mass. It was also reported that the deposit loses mass and is no longer hygroscopic after irradiation by solar UV radiation.

Quantitative description of the gaseous combustion products for high altitude rockets using bi-propellant varies depending on the engine size, its performance characteristics, and the location in the exhaust plume. There are higher concentrations of heavy species near the plume axis, and light species near the outer edge of the plume. A collection of exhaust plume composition obtained from several sources is listed in Table 1.2. The variation of data demonstrates very clearly the need for extra caution in selecting the proper mixture of combustion products for any specific engine.

## 2.0 ANALYTICAL APPROACH

### 2.1 Molecular Transport at LEO

There are several modes of transport for molecular contaminants in the Low Earth Orbit (LEO) environment. The most important mode is direct transport along the line of sight. This direct transport can be analyzed using the radiation analogy. In addition, there are indirect modes of transport such as reflection and re-emission of contaminants from spacecraft surfaces, and the scattering of contaminant molecules with other contaminant molecules or with ambient molecules. The mechanisms for this last mode of transport are more complicated and are most difficult to analyze.

Several analytical tools are available to analyze molecular contaminant transport. The theoretical basis for these codes is the BGK molecular scattering method derived from kinetic theory of gases[7-9]. Using the nearly free molecule flow approximation, Robertson[10] simplified the basic equations, and obtained approximate solutions for analyzing self contamination of convex spacecraft due to return flux of outgassed molecules. Based on this method, Wang developed the molecular scattering code (MOLESCAT)[11,12], which has been used in numerous spacecraft contamination analyses. In the ensuing years, Wang has added additional capabilities, including calculations of number densities[13,14] and treatment of multiple scattering for dense outgas cloud[15]. The same methodology has been used for the other contamination codes including the SPACE-II code[16] and the MOLFLUX code[17].

The basic assumptions used in the return flux analysis can be summarized as follows:

- The outgas cloud can be modeled as free molecule flow from numerous free expansion sources having Lambertian distribution.
- There are sufficient molecules in the contaminant cloud so that meaningful mean gasdynamic properties of number density, mean velocity, and kinetic temperature can be defined.
- The flow regime is assumed to be near free molecule flow, with the return flux a small perturbation of the basic outgas flow.
- The return flux to the critical surface is due either to scattering among the outgas molecules, or to scattering with the ambient molecules.
- The effects on the velocity distribution function due to these collisions can be separated and can be modeled by the BGK relaxation model for binary mixtures.
- The return fluxes are obtained by numerical integration of the resulting equations [12,18].

## 2.2 Plume Flowfield Description

The characteristics of high altitude plume contain detailed structure. In the near field, the engine exhaust still retains the effects of the nozzle. The flow may have an inviscid core where the flow is not affected by the ambient condition. There is the viscous layer where the effects of nozzle boundary layer dominates. A mixing layer exists where the ambient flow and the jet interact. There may also be shock waves and expansion fans to allow for pressure equilibration between the exhaust plume and the ambient. A transition region follows in which the flow adjusts itself to the ambient condition. Finally, in the far field, the flow becomes fully expanded and loses its influence from the engine nozzle. In this far field, the flow can be represented as issued from a point source. Figure 2.1 shows the different regions of a typical plume.

The flow field properties of a high altitude rocket plume can be generated using the method of characteristics (MOC) of continuum mechanics. The VOFMOC program[19] solves inviscid supersonic rocket exhaust flow equations with variable oxygen-to-fuel ratio. A two-phase plume code, the RAMP program[20], has the capability of calculating droplet/solid trajectories. These codes have been used to provide plume flowfield description of rocket exhaust in the atmospheric environment, and to predict plume impingement force and momentum on spacecraft components[21]. Another plume contamination computer code using the continuum mechanics approach is the CONTAM code[22].

Since the plume flow field encompasses continuum, transitional, and rarefied flow regimes, the continuum method breaks down when the mean free path of the flow is large compared to the characteristic length. For flows in this region, a numerical simulation method developed by Bird[23] is used. This method, called Direct Simulation Monte Carlo (DSMC), requires extensive computer time and model setup time. It has been used primarily to study the physical details of the molecular interactions. It is especially suitable for analyzing non-equilibrium flows involving internal degrees of freedom.

A comparison of DSMC and RAMP calculations of PRCS plume flowfield was reported recently[24]. The result indicated that the DSMC model[25] under-predicts the continuum model at the outer region of the plume. Hence any analytical model based on results of continuum analysis should provide conservative estimates to the contamination transport in the same regions.

In engineering analysis, for which quick turnaround time is desired, simplified plume models have been used. The plume flow field is usually assumed to be symmetric, and its flow properties are expressed in terms of its distance from the nozzle exit and the angle from the nozzle centerline. Scaling laws obtained from experimental results were used to formulate the analytical functional. Numerical results from either the continuum methods or the DSMC method are used to fit the functional and provide the necessary coefficients. This approach provides an analytical tool for quick results. However, the accuracy of the results depends heavily on the functional and the data used. The plume models used in the SPACE code and the MOLFLUX code belong to this category.

## 2.3 Contamination Analysis Tools

Analytical tools for contamination prediction have been developed by government and industry to assist in designing space instruments and in making mission planning decisions. Several molecular transport analysis codes are available based on the BGK

relaxation model, as stated previously. Models for predicting rocket plumes in a space environment are also available.

Analysis tools for contamination effects on optical elements are also available. An example is the thin film code for analyzing the throughput of optical signals through multiple layers of surface-deposited contaminants. Table 2.1 gives a representative list of gasdynamic and contamination analysis tools used in the industry.

## **2.4 Operations of the MOLFLUX Code**

The computer code used in this investigation is MOLFLUX, Rev. 2. This code was developed by NASA JSC with help from various contractors. The version that we used was obtained from Boeing Aerospace Company located in Huntsville. This program was loaded and executed using the MAPTIS VAX computer located at Marshall Space Flight Center.

The MOLFLUX code is a comprehensive computer code which can be used to calculate deposition by direct flow, reflection and re-evaporation from spacecraft surfaces, return flux, and column densities, all in one program. To operate this code, the program requires several permanent files to be attached in the run stream. These files cover ambient number density based on altitude and solar activities, data on material outgas rates, surface temperature data, view factor data, and plume flowfield models. Table 2.2 gives a list of the default datafiles and their contents.

The program uses NAMELIST input for parameters and variables. In Revision 2, a MENU option was introduced, allowing the user to review the input parameters, logic flags, and datafiles; make modifications; and submit batch runs. It is a program that requires a great deal of familiarity prior to its usage. It has a detailed User's Manual which includes 104 pages of instructions on using the MENU option, and 30 pages of instructions on NAMELIST input.

The MOLFLUX code has a built-in geometry datafile for Space Station Freedom. Executing MOLFLUX for other problems requires overriding the default datafiles, and setting the numerous logic flags to their proper values. It also requires using a geometry file and two view factor files with data format compatible to the output file of a TRASYS[26] run.

To analyze the PRCS return flux, a model for the Astro-2 payload together with the nine +Z firing PRCS was first built, and a TRASYS run was made with the RTHETO option to generate the necessary output file. With this output file, appropriate input files for MOLFLUX were then obtained. Using these datafiles, MOLFLUX runs for return flux calculation were then executed.

## 3.0 RESULTS AND DISCUSSION

### 3.1 PRCS Return Flux

The return flux from the +Z firing PRCS thrusters was calculated using the MOLFLUX code. The PRCS plume flowfield description using the 15-zone patch model[27] was included in the datafile of the code. The application points given in Table 1.1 are used as the sources of the plumes. All PRCS engines were assumed to be firing in the +Z direction with exhaust plumes consisting of one percent unburned fuel. The critical surfaces are the apertures of the Astro-2 instruments, pointing in the +Z direction, with FOVs of 90 degrees. Since the exact locations of the Astro-2 instruments are still unknown, the locations of the Astro-1 mission instruments were used in this analysis.

For ambient scattering return flux, the ambient conditions at an orbital altitude of 350 km were used. Using an average ambient number density at medium solar spot activities, and a typical ambient flow velocity of 7.8 km/sec, ambient scattering return fluxes were calculated for several Orbiter orientations. Results are presented for the Orbiter flying with nose in the RAM direction and with the payload bay in the RAM direction.

Return flux results using MOLFLUX code are presented in Tables 3.1 through 3.9. Tables 3.1 through 3.3 give self scattering return flux of H<sub>2</sub>O, unburned fuel, and total return flux of all exhaust species due to each PRCS firing individually. Same data for ambient scattering are given in Tables 3.4 through 3.9. Data listed are in units of grams of returned species per unit area of critical surface per unit time.

The results can be summarized as follows:

- Self scattering return flux dominates over ambient scattering return flux for the current problem.
- The instruments are clustered, so return flux results are within 10% of each other.
- Return flux from engines that are clustered are nearly identical.
- Returned water molecules are of the order of  $5 \times 10^{-10}$  gm/cm<sup>2</sup>/sec.
- Unburned fuel returned to instruments at the rate of  $1 \times 10^{-11}$  gm/cm<sup>2</sup>/sec.

The ambient scattering return flux depends on the Orbiter flight orientation. A comparison of results given in Tables 3.4 through 3.6 with those in Tables 3.7 through 3.9 shows that the ambient return flux with payload bay in the RAM direction is approximately two orders of magnitude higher than those with the Orbiter nose in the RAM direction. Results for the orientation with an Orbiter wing flying in the RAM direction are similar to those with Orbiter nose in the RAM direction.

### 3.2 Column Density Results

Efforts to calculate column density using MOLFLUX code were initially unsuccessful. After several tries, the program still would not execute. Due to time

constraints, this effort had to be terminated, and column density results were obtained using the BGK model approximation described in Ref. [14].

Table 3.10 presents column densities along the +Z direction LOS for three representative PRCS: F2U, F3U, and R4U. The results indicate that column densities along the +Z direction due to any PRCS firings are within 20 percent of each other. It is also shown that column densities due to ambient scattering could be much higher than those from self scattering.

Table 3.11 presents the maximum column densities over the hemi-spherical space seen by the Astro instruments. By comparison, these numbers are much higher than those given in Table 3.10. This indicates that the maximum column densities lie in directions away from the +Z LOS. This is true because the PRCS engines under consideration are over 500 inches away from the Astro-2 instruments. If the FOVs for the Astro-2 instruments are limited to smaller angles, the column density from these PRCS firings will have minimum impact to the Astro-2 observations.

During the final preparation of this document, additional MOLFLUX calculations were conducted and column density results were obtained. Tables 3.12 through 3.14 present column densities for H<sub>2</sub>O, CO<sub>2</sub>, and total plume exhaust products along +Z direction for each PRCS firing. These results look reasonable and compare well with the BGK results. Due to the limited time available, detailed review of these column density results is not performed. Analysis of these data and any other results shall be conducted in a follow-on task.

### **3.3 Effects of Deposition on Instruments**

To fully understand the potential hazard of PRCS plumes to the Astro-2 instruments, other factors need to be considered. These are the sticking coefficients for the returned species, and the optical system performance degradation due to contaminants.

The percentage of molecules arriving at a surface and remaining on the surface can be represented by a sticking coefficient. The value of the sticking coefficient depends on surface properties and surface temperature. With the exception of highly reactive chemicals, such as the unburned fuel, the majority of the returned molecules may re-evaporate under the condition of near vacuum. Water will condense at temperatures below its freezing temperature, causing performance degradation of the optical element. Keeping the critical surfaces at a relatively warm temperature will usually eliminate this problem.

The return flux results obtained in this analysis are valid for an optical surface with an FOV of 90 degrees. Actual flight hardware usually includes such equipment as aperture doors, baffles, or shades which reduce the FOV to a much smaller value. Hence the results given here should be considered as conservative estimates.

Data collected from the recent Shuttle Plume Impingement Experiment (SPIE) [28] indicate little or no detectable deposit from PRCS engine plume on typical spacecraft surfaces at temperatures between 300 and 320°K. In a related laboratory study, more than 99.9% of hydrated MMH-NO<sub>3</sub> deposited were removed by oxygen atoms in the presence of UV/VUV. The experiment data indicates a sticking coefficient of 0.01. It also indicates that re-evaporation and atomic oxygen cleaning could further reduce the contamination deposition.

The accumulation of condensed contaminants on a typical Astro-2 optical surface may be estimated using the worst case scenario of having the payload bay pointing in the RAM direction. Assuming a sticking coefficient of 0.01, the estimated rates of deposition due to the firing of a single +Z direction PRCS are: 0.07 Å per second for H<sub>2</sub>O, 0.002 Å per second for the unburned fuels, and 0.24 Å per second for the total returned species. These deposition rates could change if more than one engine is fired. The total accumulation of contaminants during the mission, however, depends on the PRCS firing sequence, the orientation during the PRCS firings, the design, the material, and the temperature history of the Astro-2 optical instruments.

Knowledge of the instrument performance is required to define contamination effects. Contamination deposition on optical surfaces may cause either reduction in signal throughput or loss of image resolution. Transmission loss analysis or surface scattering analysis requires characterization of deposited contaminants. Additional analyses are needed to determine the effects of the contaminants on the performance of the Astro instruments.

## 4.0 LESSONS LEARNED AND RECOMMENDATIONS

### 4.1 Lessons Learned in MOLFLUX Operations

The MOLFLUX code uses 14 default datafiles which are tailored for Space Station Freedom. To analyze a different problem requires the generation of several datafiles for the new geometry model. Generation of these datafiles takes a substantial amount of time. In planning future tasks, it is necessary to include the lead time needed to obtain these datafiles.

Parametric analysis is needed to obtain better estimates of the contamination environment. A major concern in contamination analysis is the confidence level of the results. Accuracy of the results depends on the numerical scheme used in the code and the input data used in the model. It is recommended that a sensitivity analysis be performed to establish these criteria.

There were some difficulties in trying to execute the MOLFLUX code through remote terminals. This includes the incompatibility of the keyboard layout with the editing instructions used in the MENU option. There were also occasions when the user was uncertain as to whether the datafile had been updated. A more user-friendly operation will enhance the usefulness of this code.

### 4.2 Recommendation for Future Studies

To satisfy the system performance requirements of the mission, contamination control using a systematic approach is needed. By analyzing the end-to-end flow of instruments, the causes for contamination generation and transport can be identified. Using proper process control at the appropriate time in the flow, the risk of contamination hazard can be reduced.

This study is limited to contamination hazard due to Orbiter PRCS plumes only. There may be other contamination sources that can cause performance degradation to the Astro-2 instruments. This includes Orbiter Payload bay contamination sources and ground processing contamination sources generated during testing, integration, and launch operations. Analysis of contamination hazard due to these sources is outside the scope of this study. To support establishing an end-to-end contamination control plan, additional contamination analyses for these other sources are needed.

Current data on contamination effects on optics surface in the UV wavelength region is very limited. Data from Ref. 1 showed strong transmittance and reflectance degradation for wavelengths less than  $0.4 \mu\text{m}$  on selected optical surface due to MMH- $\text{HNO}_3$ . However, degradation effects on other optical surfaces are still lacking. Since more flight experiments are planned in the UV wavelength region, a broader database on optical effects due to PRCS plume products will be needed. This effort will tremendously enhance future mission planning and data analysis.

There is an apparent lack of knowledge on the effects of the space environment on contamination deposition. Evidences from previous STS flights indicate the removal of contaminants on surfaces in the RAM-facing direction. Speculations on the cause have been forwarded as due either to the reaction of atomic oxygen, to UV radiation, or both.

Systematic experiments, conducted in a controlled flight environment or in a ground simulation facility, are needed to firmly establish the cause for these observations.

In summary, additional work in the following areas is recommended:

1. Conduct an independent validation and verification task of the current MOLFLUX code.
2. Extend this analysis to include other contamination sources in order to support establishing an end-to-end contamination control plan.
3. Conduct additional data search and laboratory testing to better understand the contamination effects on optical surfaces at the UV wavelength region.
4. Conduct further experiments, both in-flight and ground, on AO and UV/VUV effects to better understand the effects on contamination deposit due to the space environment.

## REFERENCES

1. Liu, C. K. & A. P. M. Glassford, "Contamination Effect of MMH/N<sub>2</sub>O<sub>4</sub> Rocket Plume Product Deposit," J Spacecraft, Vol. 18, No. 4, July-August 1981, pp 306-311.
2. Trinks, H, "Plume Contamination TUHH Experimental Investigation, Final Report, Part 1: Experimental Results," Technical University of Hamburg Harburg, Contract No. 11-880070-39, July 1989,
3. Alt, R.E., et. al., "Bipropellant Engine Plume Contamination Program, Volume I," AEDC-TR-79-28, December 1979.
4. Powell, H.M., Price, L.L., and Alt, R.E., "Bipropellant Engine Plume Contamination Program, Volume II," AEDC-TR-79-28, November 1979.
5. Passamaneck, R. S., and J. E. Chirivella, "Small Monopropellant Thruster Contamination Measurement in a High-Vacuum Low-Temperature Facility," J. Spacecraft, Vol. 14, No 7, July 1977, pp. 419 - 426.
6. Guernsey, C.S., and R.D. McGregor, "Bipropellant Rocket Exhaust Plume Analysis on the Galileo Spacecraft," AIAA-86-1488, June 1986.
7. Bhatnagar, P.L., E.P. Gross and M. Krook, "A Model for Collision Processes in Gases-I. Small Amplitude Processes in Charged and Neutral One-Component Systems," Phys. Rev. Vol. 94, No. 3, May 1954, pp. 511-525.
8. Hamel, B.B., "Kinetic Model for Binary Gas Mixtures," Phys. Fluids, Vol. 8, No. 3, March 1965, pp. 418-425.
9. Morse, T.F., "Kinetic Model Equations for a Gas Mixtures," Phys. Fluids, Vol. 7, No. 12, December 1964, pp. 2021-2013.
10. Robertson, S.J., "Bhatnagar-Gross-Krook Model Solution of Back-Scattering of Outgas Flow from Spherical Spacecraft," in Rarefied Gas Dynamics (J.L. Potter, ed.), American Institute of Aeronautics and Astronautics, New York, 1977, pp.479-489.
11. Wang, F.C., "A BGK Model Study of Spacecraft Self-Contamination, Volume I, Theory and Application, and Volume II, MOLESCAT User's Manual," LMSC-HREC TR D697965-I and -II, Lockheed Missiles & Space Company, Huntsville, AL. June 1980.
12. Wang, F.C., "A Molecular Scattering Model for Spacecraft Contamination Studies, Volume II, MOLESCAT2 User's Manual," LMSC-HREC TR D867306-II, Lockheed Missiles & Space Company, Huntsville, AL. January 1984.
13. Wang, F.C., "Molecular Scattering Return Flux to CIRRIS Payload From Various Orbiter and Payload Contamination Sources," LMSC-HEC TN D784628, Lockheed Missiles & Space Company, Huntsville, AL. October 1981.
14. Wang, F.C., "Number Density and Column Density Along LOS from Continuous Fluid Leakage," IDC, Lockheed Missiles & Space Co., Huntsville, AL, October 1983.

15. Wang, F.C., "A Kinetic Model for Spacecraft Self-Contamination from Moderately Dense Outgas Cloud," LMSC-HREC TR D784756, Lockheed Missiles & Space Company, Huntsville, AL. January 1982.
16. "Shuttle/Payload Contamination Program, Version II, The SPACE II Computer Program User's Manual," Final Report, MCR-80-593, Martin Marietta Company, September 1980
17. "MOLFLUX Molecular Flux User's Manual," Rev. 2, JSC-22496, NASA Johnson Space Center, July 1992.
18. Ma, P.T., L.C. Zumwalt, F.C. Wang, and S.C. Yfantis, "BGK Contamination Model of the MSX Satellite and Comparison with Monte-Carlo Simulation Data," Paper No. 1754-25, Presented at SPIE's 1992 International Symposium on Optical Applied Science and Engineering, San Diego, July 1992.
19. Smith, S.D. and A.W. Ratliff, "User's Manual - Variable O/F Ratio Method of Characteristics Program for Nozzle and Plume Analysis," LMSC-HREC D162220-IV, Lockheed Missiles & Space Company, Huntsville, AL, June 1971.
20. Smith, S.D. "High Altitude Chemical Reacting Gas Particle Mixtures," LMSC-HREC D867400-I, Lockheed Missiles & Space Company, Huntsville, AL, October 1984.
21. Smith, S.D., "Development of a Nozzle/Plume and Plume Impingement Code," CIFR008, Continuum, Inc., Huntsville, AL November 1986.
22. Hoffman, R.J. et. al., "Plume Contamination Effects Prediction - The CONTAM Computer Program, Version II," McDonnell Douglas Astronautics Co., AFRPL-TR-73-46. August 1973.
23. Bird, G.A., Molecular Gas Dynamics, Oxford University Press, 1976.
24. Smith S. D., "Estimated Accuracy of Method of Characteristics Viscous Plume Solutions for On-Orbit Plume Induced Environment Predictions," AIAA 91-1364, June 1991.
25. Hueser, J.E., and F.J. Brock, "Plume Flowfield Analysis of the Shuttle Primary Reaction Control System (RCS) Rocket Engine," Final Report for Cooperative Agreement NCC 1-94, Old Dominion University Research Foundation, Norfolk, VA, January 1990.
26. "Thermal Radiation Analysis System, TRASYS II User's Manual," June 1983.
27. Kirshman, D.J., and R.J. Rader, "Plume Flow Field Models of Space Station Thrusters and Orbiter PRCS Thrusters Using the Patch Fit Technique," McDonnell Douglas Aerospace Document MDC-9280184, April 1992.
28. Koontz, S., H. Ehlers, M. Pedley, C. Hakes, J. Cross, "Shuttle Primary Reaction Control System (PRCS) Engine Exhaust Plume Contamination Effects: The Shuttle Plume Impingement Experiment (SPIE), STS-52," AIAA Paper 93-0618, January 1993.

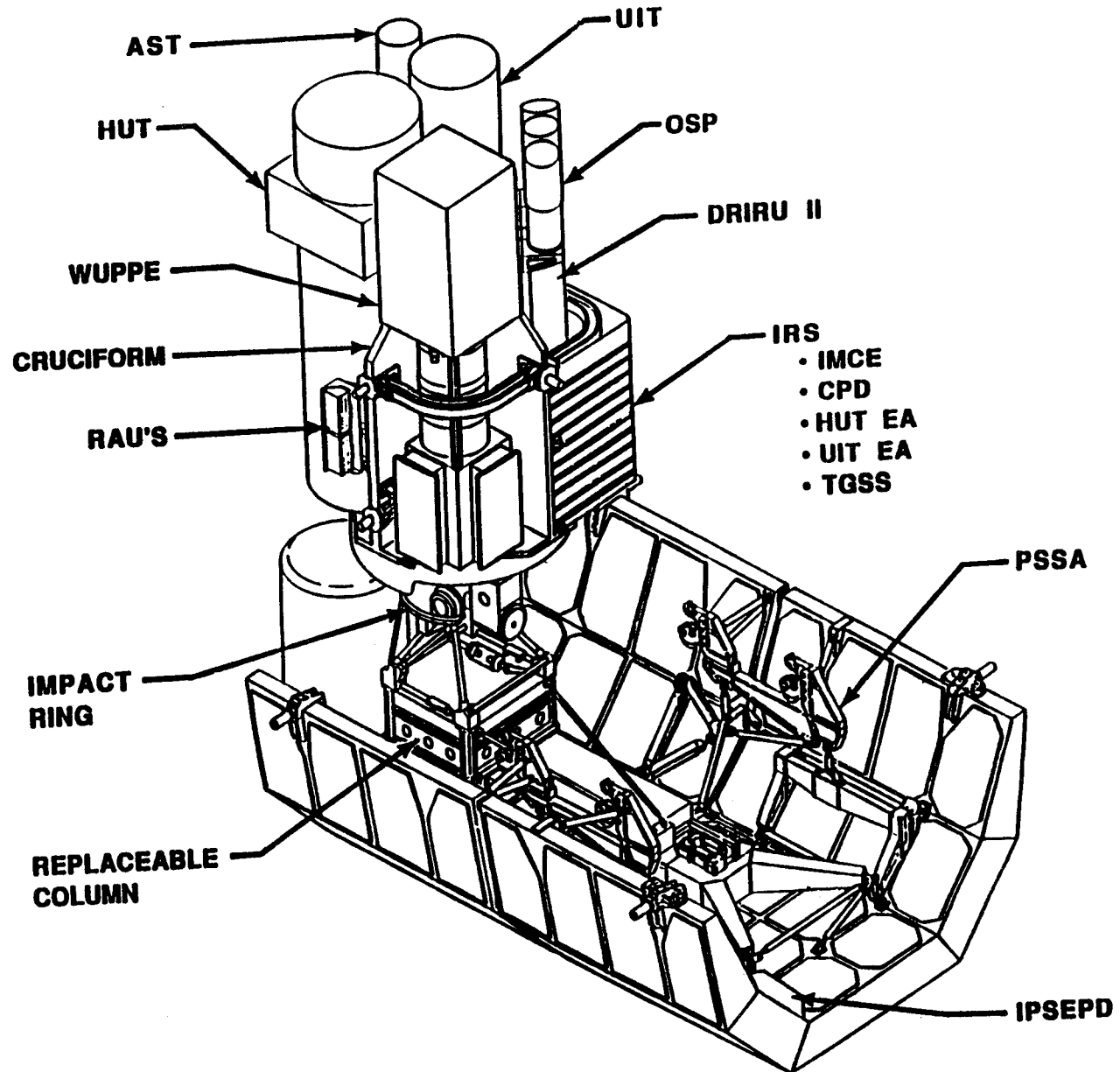
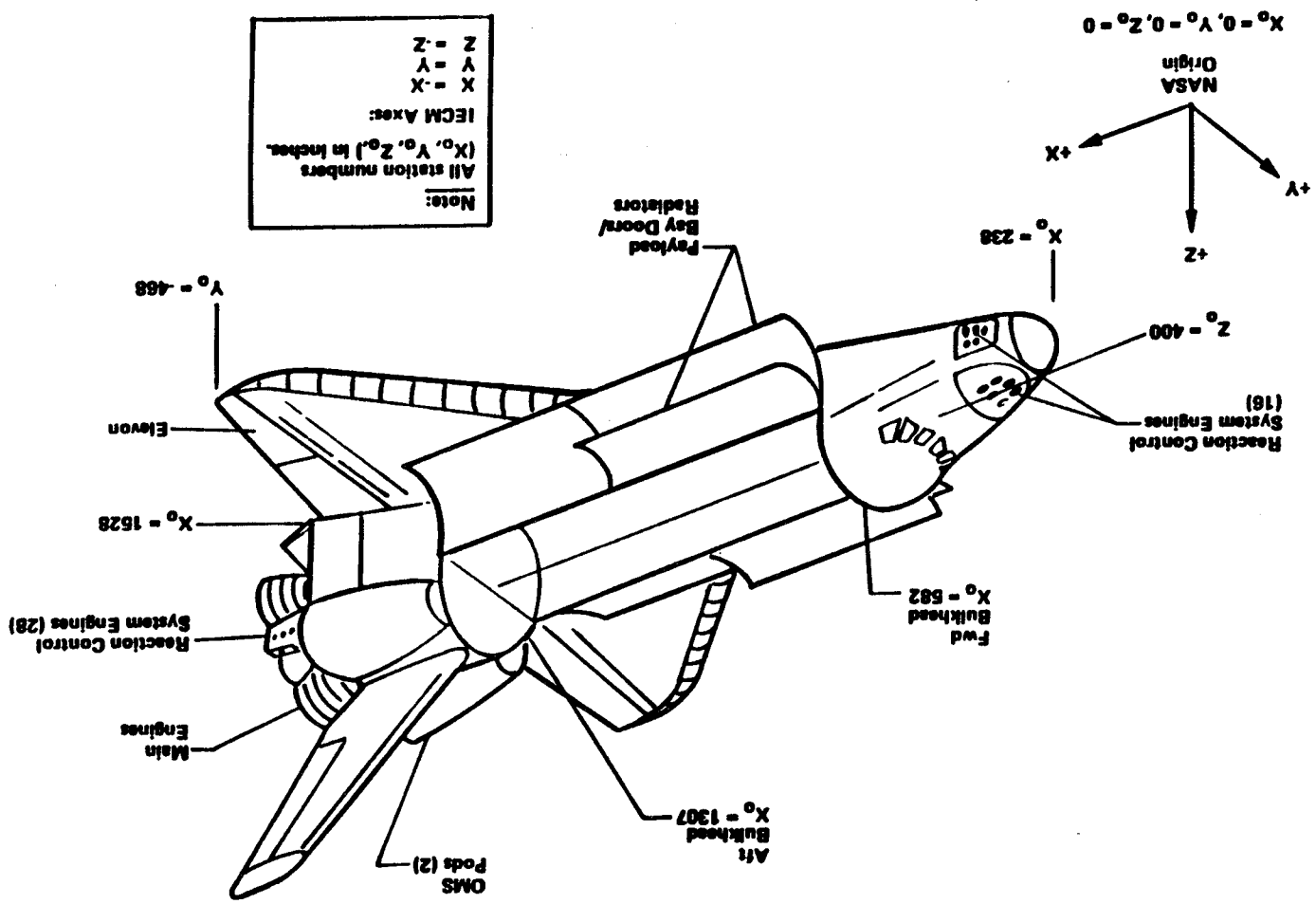
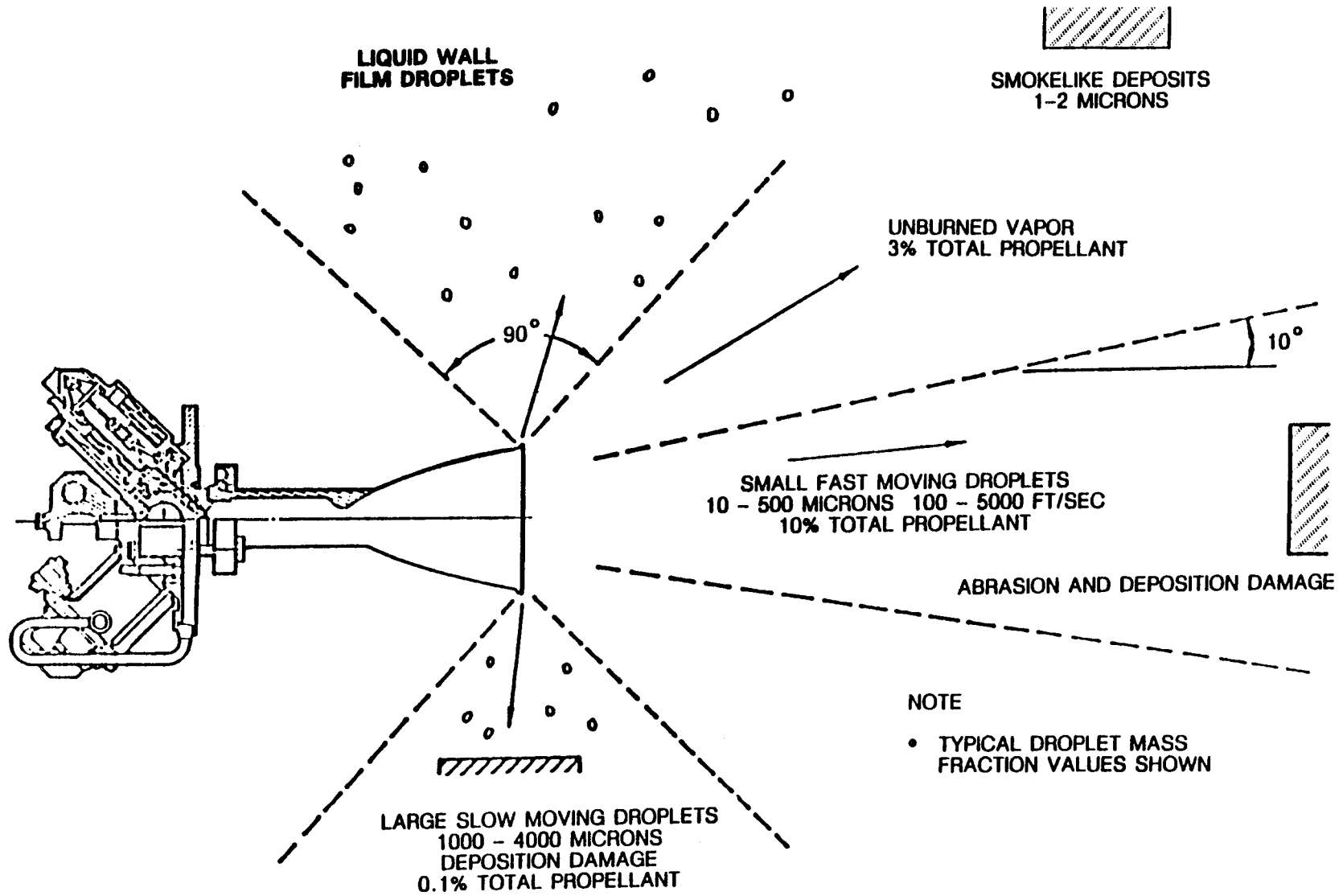


Figure 1.1 ASTRO-2 PAYLOAD CONFIGURATION

Figure 1.2 SHUTTLE ORBITER CONFIGURATION AND COORDINATES



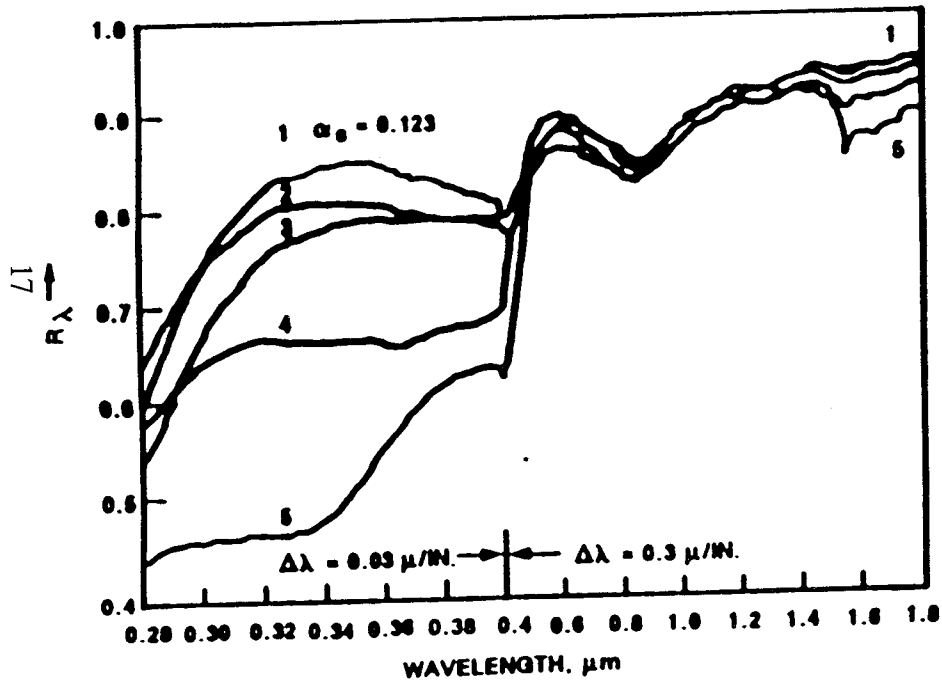




**Figure 1.4 PLUME CONTAMINATION DAMAGE**

**SPECTRAL REFLECTANCE OF MMH-HNO<sub>3</sub> LIQUID DEPOSIT ON Al MIRROR**

1. CLEAN FIRST SURFACE Al MIRROR WITH MMH-HNO<sub>3</sub> DEPOSIT OF
2.  $1.0 \times 10^{-4}$  G/CM<sup>2</sup>  $\alpha_0 = 0.124$
3.  $3.3 \times 10^{-4}$  G/CM<sup>2</sup>  $\alpha_0 = 0.135$
4.  $1.0 \times 10^{-3}$  G/CM<sup>2</sup>  $\alpha_0 = 0.15$
5.  $3.3 \times 10^{-3}$  G/CM<sup>2</sup>  $\alpha_0 = 0.76$



**SPECTRAL TRANSMITTANCE OF MMH-HNO<sub>3</sub> LIQUID DEPOSIT ON FUSED SILICA**

1. CLEAN FUSED SILICA DISC WITH MMH-HNO<sub>3</sub> DEPOSIT OF
2.  $1.0 \times 10^{-4}$  G/CM<sup>2</sup>  $T_0 = 0.921$
3.  $3.3 \times 10^{-4}$  G/CM<sup>2</sup>  $T_0 = 0.919$
4.  $1.0 \times 10^{-3}$  G/CM<sup>2</sup>  $T_0 = 0.917$
5.  $3.3 \times 10^{-3}$  G/CM<sup>2</sup>  $T_0 = 0.894$

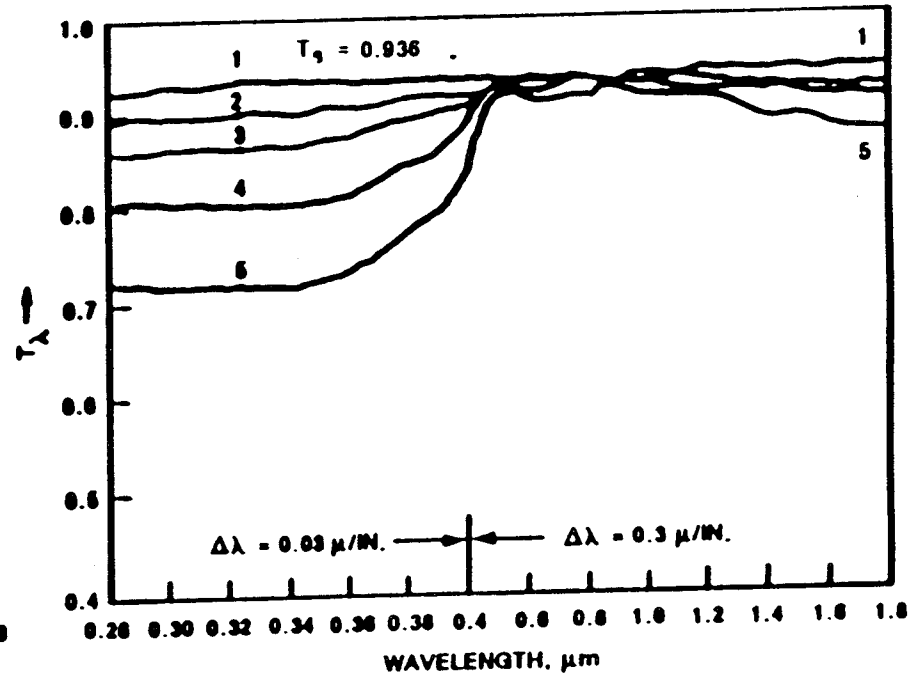


**Figure 1.5 EFFECTS OF MMH-HNO<sub>3</sub> DEPOSIT ON SELECTED OPTICAL SURFACES**

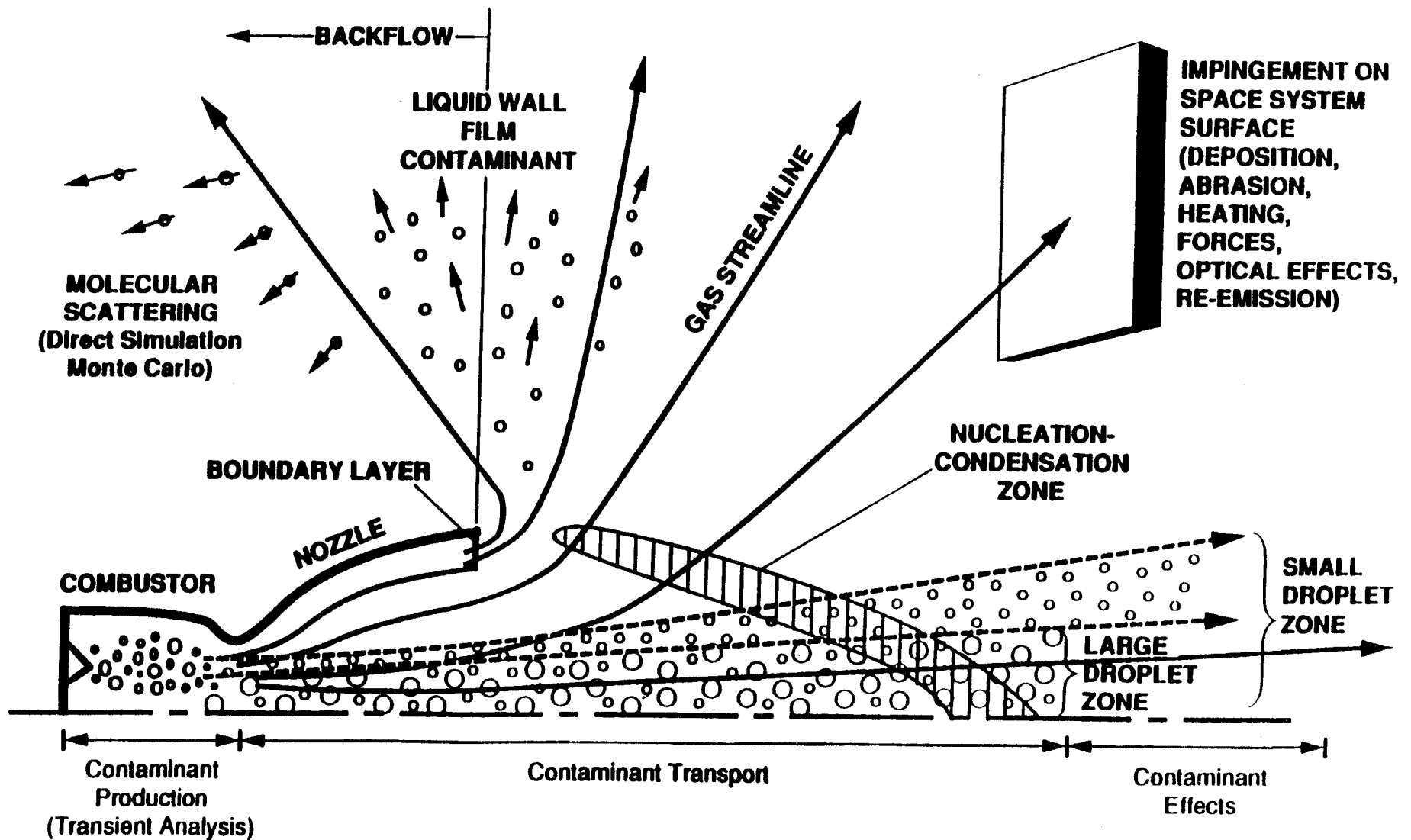


Figure 2.1 TYPICAL PLUME FLOWFIELD REGIONS

Table 1.1 NOMINAL COMPONENTS AND APPLICATION LOCATIONS

Thruster number	Thrust components, lb <sup>a,c</sup>			Resultant <sup>c</sup> thrust. lb	Thrust application <sup>b</sup>		
	F <sub>X<sub>B</sub></sub>	F <sub>Y<sub>B</sub></sub>	F <sub>Z<sub>B</sub></sub>		X <sub>0</sub>	Y <sub>0</sub>	Z <sub>0</sub>
F2F	-879.4	-26.2	119.9	887.9	306.72	14.65	392.96
F3F	-879.5	0.0	122.7	888.0	306.72	0.0	394.45
F1F	-879.4	26.2	119.9	887.9	306.72	-14.65	392.96
F1L	-26.3	873.6	18.2	874.2	362.67	-69.50	373.73
F3L	-21.0	870.3	0.5	870.6	364.71	-71.65	359.25
F2R	-26.3	-873.6	18.2	874.2	362.67	69.50	373.73
F4R	-21.0	-870.3	0.5	870.6	364.71	71.65	359.25
F2U	-32.3	-11.3	874.4	875.1	350.93	14.39	413.46
F3U	-31.9	0.0	873.5	874.1	350.92	0.0	414.53
F1U	-32.3	11.7	874.4	875.1	350.93	-14.39	413.46
F2D	-28.0	-616.4	-639.5	888.6	333.84	61.42	356.95
F1D	-28.0	616.4	-639.5	888.6	333.84	-61.42	356.95
F4D	-24.8	-612.6	-639.4	885.9	348.44	66.23	358.44
F3D	-24.8	612.6	-639.4	885.9	348.44	-66.23	358.44
F5R	-0.8	-17.0	-17.6	24.5	324.35	59.70	350.12
F5L	-0.8	17.0	-17.6	24.5	324.35	-59.70	350.12
R3A	856.8	0.0	151.1	870.0	1555.29	137.00	473.06
R1A	856.8	0.0	151.1	870.0	1555.29	124.00	473.06
L3A	856.8	0.0	151.1	870.0	1555.29	-137.00	473.06
L1A	856.8	0.0	151.1	870.0	1555.29	-124.00	473.06
L4L	0.0	870.5	-22.4	870.8	1516.00	-149.87	459.00
L2L	0.0	870.5	-22.4	870.8	1529.00	-149.87	459.00
L3L	0.0	870.5	-22.4	870.8	1542.00	-149.87	459.00
L1L	0.0	870.5	-22.4	870.8	1555.00	-149.87	459.00
R4R	0.0	-870.5	-22.4	870.8	1516.00	149.87	459.00
R2R	0.0	-870.5	-22.4	870.8	1529.00	149.87	459.00
R3R	0.0	-870.5	-22.4	870.8	1542.00	149.87	459.00
R1R	0.0	-870.5	-22.4	870.8	1555.00	149.87	459.00
L4U	0.0	0.0	870.0	870.0	1516.00	-132.00	480.50
L2U	0.0	0.0	870.0	870.0	1529.00	-132.00	480.50
L1U	0.0	0.0	870.0	870.0	1542.00	-132.00	480.50
R4U	0.0	0.0	870.0	870.0	1516.00	+132.00	480.50
R2U	0.0	0.0	870.0	870.0	1529.00	132.00	480.50
R1U	0.0	0.0	870.0	870.0	1542.00	132.00	480.50
L4D	170.4	291.8	-801.7	870.0	1516.00	-111.95	437.40
L2D	170.4	291.8	-801.7	870.0	1529.00	-111.00	440.00
L3D	170.4	291.8	-801.7	870.0	1542.00	-110.06	442.60
R4D	170.4	-291.8	-801.7	870.0	1516.00	111.95	437.40
R2D	170.4	-291.8	-801.7	870.0	1529.00	111.00	440.00
R3D	170.4	-291.8	-801.7	870.0	1542.00	110.06	442.60
L5D	0.0	0.0	-24.0 <sup>d</sup>	24.0 <sup>d</sup>	1565.00	-118.00	445.44
R5D	0.0	0.0	-24.0 <sup>d</sup>	24.0 <sup>d</sup>	1565.00	118.00	455.44
L5L	0.0	24.0	-0.6	24.0	1565.00	-149.87	459.00
R5R	0.0	-24.0	-0.6	24.0	1565.00	149.87	459.00

**Table 1.2 MOLE FRACTION OF ENGINE EXHAUST**

Species	10 N Engine		Experiment	Trinks *		PRCS	
	Theoretical	Hypothetical		ODE	Max Transient	MOLFLUX	MOC
CO	0.174	0.164	~0.100	0.110	0.100	0.184	0.1189
CO <sub>2</sub>	0.088	0.083	0.060	0.060	0.060	0.078	0.0495
H	0.002	0.001	~0.010	0.001	0.050	0.001	0.0095
H <sub>2</sub>	0.015	0.014	0.180	0.180	0.400	0.017	0.1637
H <sub>2</sub> O	0.298	0.281	0.300	0.340	0.300	0.290	0.3311
NO	0.003		~0.010	0.000	0.100		
N <sub>2</sub>	0.418	0.397	~0.300	0.310	0.200	0.420	0.3097
OH	0.001		~0.010	0.001	0.050		0.0113
O <sub>2</sub>	0.001		~0.010	0.000	0.100	0.001	0.0027
O						0.002	0.0012
HCN			~0.010		0.050		
HCO			~0.005		0.050		
NO <sub>2</sub>			~0.005		0.050		
MMH		0.025					
HNO <sub>3</sub>		0.035					

\* FROM TRINKS: "Plume Contamination: TUHH Experimental Investigation, Final Report, Part 1. .  
Experimental Results." 20 July 1989.

**Table 2.1 GASDYNAMIC AND CONTAMINATION ANALYSIS TOOLS**

**COMPUTER CODE**

1) MOLECULAR TRANSFER KINETICS FREE MOLECULAR (MTK)

2) MOLECULAR TRANSPORT WITH INTERMOLECULAR COLLISIONS MONTE CARLO (MCTK) DIFFUSION (SPAR)

3) ROCKET EXHAUST THERMO-CHEMISTRY AND NOZZLE FLOW (ODK, TDK, CONTAM 3)

4) PLUME IMPINGEMENT EFFECTS (MOC, RAMP, PLIMP)

5) MOLECULAR SCATTERING (MOLESCAT)

6) MOLECULAR FLUX (SPACE, MOLFLUX)

7) PLUME BACKFLUX (GAPS, BKFLW)

8) DEPOSIT-INCLUDED SURFACE CHANGE

9) MIE SCATTERING (MIESC) SCATTERING DIFFRACTION (LIESCA)

10) THIN FILM OPTICS CODE

**FUNCTIONS AND CAPABILITIES**

- CONTAMINATION FLUX TRANSPORT IN SPACE ENVIRONMENT
- RADIATIVE HEATING ANALOGY
- SURFACE/GAS INTERACTION PHENOMENA
- DEPOSIT FLUX AND TOTAL DEPOSITION

- CONTAMINANT TRANSPORT IN NEAR FREE-MOLECULE ENVIRONMENT
- MONTE CARLO SIMULATION OR DIFFUSION
- SURFACE/GAS INTERACTION PHENOMENA SAME AS MTK

- THERMAL CHEMICAL EQUILIBRUM AND KINETICS
- NOZZLE FLOW CHARACTERIZATION
- GAS AND MULTI-PHASE FLOW

- METHOD-OF-CHARACTERISTICS
- TWO-PHASE FLOW; NOZZLE VISCOUS EFFECTS
- PLUME FLOWFIELD AND IMPINGEMENT PROPERTIES

- MOLECULAR BACKSCATTER OF OUTGASSED SPECIES
- BGK BINARY COLLISION MODEL USED;
- USES POINT SOURCE APPROXIMATION
- CALCULATES RETURN FLUX AND COLUMN DENSITY

- CALCULATES DIRECT FLUX, RETURN FLUX, COLUMN DENSITY
- USES BGK MODEL
- USES VIEW FACTOR DATA AS INPUT

- FREE-MOLECULAR DISTRIBUTION FROM OUTER PLUME (BIRD'S CRITERION)
- MONTE CARLO SIMULATION (GAPS); SIMPLIFIED MODEL (BKFLW)

- MAXWELLS SOLUTION FOR WAVE PROPAGATION
- SUBSTRATE, COATING, AND CONTAMINATION FLUX

- LIGHT SCATTERING BY SPHERICAL OR CYLINDRICAL PARTICLES
- PARTICLE-INDUCED OPTICAL SURFACE DEGRADATION

- CALCULATES OPTICAL THROUGHPUT USING THIN FILM PROPERTIES
- CAN CALCULATE MULTI-LAYER DEPOSITIONS

**TABLE 2.2 INPUT FILE REQUIREMENTS**

<b>Default File Name</b>	<b>Logical Unit Number</b>	<b>File Format</b>	<b>File Contents</b>
GEOM-F01.DSK	1	text	list of node numbers for all surfaces, engines, vents, with description and area
RATES-F02.DSK	2	text	list of outgassing rates and species
ENGC-F03.DSK	3	text	engine characteristics; parameters for each of the 15 "zones"
ENGS-F04.DSK	4	text	locations and orientations of all concentrates sources
MATRL-F07.DSK	7	text	lists node number of all surfaces with material type of each surface
AMBDN-F08.DSK	8	text	table of atmospheric densities, accounting for low, medium, or high sunspot activity; provides the default ambient density
AMBPRG-F09.DSK	9	text	another table of atmospheric densities; calculation also includes orbital position and different species
TEMP-F10.DSK	10	text	an array of up to 25 temperatures for each node in the model
GRIDSP-F11.DSK	11	text	locations of all points in the point matrix
TAPE12.DAT	12	direct access	file containing all surface-to-surface view factors
TAPE13.DAT	13	direct access	file containing all points-to-surface view factors

**Table 3.1 SELF SCATTERING RETURN FLUX, H<sub>2</sub>O**

Amount of H<sub>2</sub>O (E-10 gm/cm<sup>2</sup>/sec)

<u>Engine</u>	<u>AST</u>	<u>HUT</u>	<u>OSP</u>	<u>UIT</u>	<u>WUPPE</u>
F1U	5.38	5.19	4.19	5.01	4.28
F2U	5.42	5.16	4.21	5.04	4.26
F3U	5.39	5.16	4.19	5.01	4.26
L1U	2.40	2.51	2.82	2.49	2.88
L2U	2.48	2.60	2.94	2.58	3.01
L4U	2.56	2.69	3.08	2.67	3.15
R1U	2.46	2.47	2.92	2.56	2.78
R2U	2.54	2.55	3.06	2.65	2.91
R4U	2.63	2.64	3.21	2.75	3.04

**Table 3.2 SELF SCATTERING RETURN FLUX, UNBURNED FUEL**

Amount of Unburned Fuel (E-12 gm/cm<sup>2</sup>/sec)

<u>Engine</u>	<u>AST</u>	<u>HUT</u>	<u>OSP</u>	<u>UIT</u>	<u>WUPPE</u>
F1U	13.3	12.9	10.5	12.5	10.8
F2U	13.4	12.8	10.6	12.6	10.7
F3U	13.3	12.8	10.5	12.5	10.7
L1U	5.80	6.11	7.06	6.07	7.22
L2U	6.02	6.37	7.40	6.31	7.59
L4U	6.26	6.65	7.78	6.58	7.98
R1U	5.97	6.00	7.35	6.26	6.91
R2U	6.21	6.23	7.72	6.53	7.32
R4U	6.47	6.50	8.13	6.82	7.68

**Table 3.3 SELF SCATTERING RETURN FLUX, TOTAL**

Amount of Total Flux (E-10 gm/cm<sup>2</sup>/sec)

<u>Engine</u>	<u>AST</u>	<u>HUT</u>	<u>OSP</u>	<u>UIT</u>	<u>WUPPE</u>
F1U	16.7	16.2	13.2	15.7	13.4
F2U	16.9	16.1	13.2	15.8	13.4
F3U	16.8	16.1	13.1	15.7	13.4
L1U	7.36	7.73	8.80	7.67	9.00
L2U	7.62	8.03	9.21	7.96	9.42
L4U	7.91	8.34	9.66	8.26	9.90
R1U	7.56	7.59	9.14	7.89	8.63
R2U	7.84	7.86	9.59	8.20	9.11
R4U	8.13	8.17	10.1	8.53	9.53

**Table 3.4 AMBIENT SCATTERING RETURN FLUX, H<sub>2</sub>O**

Amount of H<sub>2</sub>O (E-12 gm/cm<sup>2</sup>/sec)

<u>Engine</u>	<u>AST</u>	<u>HUT</u>	<u>OSP</u>	<u>UIT</u>	<u>WUPPE</u>
F1U	1.60	1.61	1.65	1.61	1.65
F2U	1.60	1.61	1.65	1.61	1.65
F3U	1.60	1.61	1.65	1.61	1.65
L1U	1.63	1.62	1.59	1.62	1.58
L2U	1.62	1.61	1.58	1.61	1.58
L4U	1.61	1.60	1.58	1.60	1.56
R1U	1.62	1.62	1.58	1.61	1.59
R2U	1.62	1.62	1.58	1.60	1.58
R4U	1.61	1.60	1.56	1.59	1.58

---

Ambient flow in +X direction  
Altitude at 350 Km with medium solar spot activities

**Table 3.5 AMBIENT SCATTERING RETURN FLUX, UNBURNED FUEL****Amount of Unburned Fuel (E-14 gm/cm<sup>2</sup>/sec)**

<b><u>Engine</u></b>	<b><u>AST</u></b>	<b><u>HUT</u></b>	<b><u>OSP</u></b>	<b><u>UIT</u></b>	<b><u>WUPPE</u></b>
F1U	5.58	5.57	5.65	5.57	5.64
F2U	5.58	5.57	5.65	5.57	5.64
F3U	5.58	5.57	5.65	5.57	5.64
L1U	5.58	5.53	5.49	5.54	5.48
L2U	5.54	5.50	5.48	5.51	5.47
L4U	5.51	5.47	5.46	5.48	5.45
R1U	5.55	5.55	5.48	5.51	5.45
R2U	5.52	5.52	5.47	5.48	5.48
R4U	5.49	5.49	5.45	5.46	5.47

---

Ambient flow in +X direction  
Altitude at 350 Km with medium solar spot activities

**Table 3.6 AMBIENT SCATTERING RETURN FLUX, TOTAL****Amount of Total Flux (E-12 gm/cm<sup>2</sup>/sec)**

<b><u>Engine</u></b>	<b><u>AST</u></b>	<b><u>HUT</u></b>	<b><u>OSP</u></b>	<b><u>UIT</u></b>	<b><u>WUPPE</u></b>
F1U	5.56	5.56	5.69	5.57	5.68
F2U	5.56	5.56	5.69	5.57	5.68
F3U	5.56	5.56	5.69	5.57	5.68
L1U	5.62	5.58	5.50	5.58	5.49
L2U	5.59	5.54	5.48	5.55	5.48
L4U	5.56	5.51	5.47	5.52	5.44
R1U	5.60	5.59	5.49	5.56	5.49
R2U	5.57	5.56	5.48	5.52	5.49
R4U	5.53	5.53	5.44	5.49	5.48

---

Ambient flow in +X direction  
Altitude at 350 Km with medium solar spot activities

**Table 3.7 AMBIENT SCATTERING RETURN FLUX, H<sub>2</sub>O**

Amount of H<sub>2</sub>O (E-10 gm/cm<sup>2</sup>/sec)

<u>Engine</u>	<u>AST</u>	<u>HUT</u>	<u>OSP</u>	<u>UIT</u>	<u>WUPPE</u>
F1U	2.18	2.19	2.16	2.19	2.17
F2U	2.05	2.08	2.07	2.08	2.07
F3U	2.05	2.08	2.06	2.08	2.07
L1U	2.34	2.19	2.22	2.19	2.22
L2U	2.18	2.20	2.24	2.20	2.24
L4U	2.19	2.21	2.24	2.21	2.24
R1U	2.18	2.18	2.23	2.19	2.22
R2U	2.19	2.19	2.24	2.20	2.23
R4U	2.20	2.20	2.24	2.21	2.24

---

Ambient flow in -Z direction  
 Altitude at 350 km with medium solar spot activities

**Table 3.8 AMBIENT SCATTERING RETURN FLUX, UNBURNED FUEL**

Amount of Unburned Fuel (E-12 gm/cm<sup>2</sup>/sec)

<u>Engine</u>	<u>AST</u>	<u>HUT</u>	<u>OSP</u>	<u>UIT</u>	<u>WUPPE</u>
F1U	7.44	7.47	7.63	7.50	7.63
F2U	6.62	6.69	7.00	6.74	7.00
F3U	6.63	6.69	7.01	6.76	7.00
L1U	7.83	7.54	7.57	7.54	7.57
L2U	7.53	7.56	7.67	7.56	7.66
L4U	7.56	7.58	7.63	7.57	7.60
R1U	7.53	7.53	7.68	7.56	7.58
R2U	7.55	7.56	7.64	7.57	7.68
R4U	7.57	7.57	7.57	7.58	7.65

---

Ambient flow in -Z direction  
 Altitude at 350 km with medium solar spot activities

**Table 3.9 AMBIENT SCATTERING RETURN FLUX, TOTAL**

Amount of Total Flux (E-10 gm/cm<sup>2</sup>/sec)

<u>Engine</u>	<u>AST</u>	<u>HUT</u>	<u>OSP</u>	<u>UIT</u>	<u>WUPPE</u>
F1U	7.50	7.53	7.57	7.56	7.59
F2U	6.90	6.99	7.11	7.02	7.11
F3U	6.91	6.99	7.10	7.03	7.11
L1U	7.96	7.56	7.64	7.55	7.64
L2U	7.54	7.59	7.72	7.58	7.72
L4U	7.58	7.62	7.72	7.61	7.70
R1U	7.53	7.54	7.72	7.58	7.63
R2U	7.57	7.57	7.72	7.61	7.72
R4U	7.60	7.60	7.69	7.63	7.72

Ambient flow in -Z direction  
 Altitude at 350 km with medium solar spot activites

**Table 3.10 COLUMN DENSITY IN +Z DIRECTION (BGK RESULTS)  
 (NO/CM<sup>2</sup>)**

	<u>AST</u>	<u>HUT</u>	<u>OSP</u>	<u>UIT</u>	<u>WUPPE</u>
<u>Self Scattering</u>					
<b>F2U</b>	6.76E+14	6.60E+14	6.33E+14	6.60E+14	6.30E+14
<b>F3U</b>	6.74E+14	6.62E+14	6.32E+14	6.59E+14	6.28E+14
<b>R4U</b>	5.04E+14	5.16E+14	5.98E+14	5.24E+14	5.71E+14
<u>Ambient Scattering</u>					
<b>F3U</b>	5.19E+16	4.97E+16	4.47E+16	4.90E+16	4.51E+16
<b>R4U</b>	5.67E+16	5.76E+16	6.39E+16	5.91E+16	6.21E+16

**Table 3.11 MAXIMUM COLUMN DENSITY (BGK RESULTS)  
(NO/CM<sup>2</sup>)**

	<u>AST</u>	<u>HUT</u>	<u>OSP</u>	<u>UIT</u>	<u>WUPPE</u>
<u>Self Scattering</u>					
<b>F2U</b>	4.32E+15	4.13E+15	3.50E+15	4.04E+15	3.64E+15
<b>F3U</b>	4.34E+15	4.11E+15	3.58E+15	4.06E+15	3.62E+15
<b>R4U</b>	2.21E+15	2.83E+15	2.55E+15	2.33E+15	2.93E+15
<u>Ambient Scattering</u>					
<b>F3U</b>	2.99E+17	3.08E+17	2.94E+17	2.97E+17	2.98E+17
<b>R4U</b>	1.39E+17	2.41E+17	1.71E+17	1.49E+17	3.41E+17

**Table 3.12 COLUMN DENSITY, H<sub>2</sub>O**

Amount of H<sub>2</sub>O (E+16 NO/CM<sup>2</sup>)

<u>Engine</u>	<u>AST</u>	<u>HUT</u>	<u>OSP</u>	<u>UIT</u>	<u>WUPPE</u>
F1U	1.36	1.35	1.24	1.33	1.25
F2U	1.36	1.34	1.24	1.33	1.25
F3U	1.36	1.35	1.24	1.33	1.25
L1U	.993	1.06	1.12	1.05	1.13
L2U	1.05	1.08	1.13	1.07	1.14
L4U	1.07	1.10	1.16	1.09	1.17
R1U	1.05	1.05	1.13	1.07	1.12
R2U	1.07	1.07	1.15	1.09	1.13
R4U	1.09	1.09	1.18	1.11	1.15

Table 3.13 COLUMN DENSITY, CO<sub>2</sub>

		<u>Amount of CO<sub>2</sub> (E+16 No/cm<sup>2</sup>)</u>			
<u>Engine</u>	<u>AST</u>	<u>HUT</u>	<u>OSP</u>	<u>UIT</u>	<u>WUPPE</u>
F1U	1.50	1.48	1.37	1.46	1.38
F2U	1.50	1.48	1.37	1.47	1.37
F3U	1.50	1.48	1.37	1.47	1.38
L1U	1.09	1.16	1.23	1.16	1.24
L2U	1.16	1.19	1.25	1.18	1.26
L4U	1.18	1.21	1.27	1.20	1.29
R1U	1.15	1.15	1.24	1.18	1.23
R2U	1.17	1.17	1.27	1.20	1.24
R4U	1.19	1.20	1.30	1.22	1.27

Table 3.14 COLUMN DENSITY, TOTAL

		<u>Total column density (E+16 No/cm<sup>2</sup>)</u>			
<u>Engine</u>	<u>AST</u>	<u>HUT</u>	<u>OSP</u>	<u>UIT</u>	<u>WUPPE</u>
F1U	4.17	4.12	3.80	4.07	3.83
F2U	4.18	4.12	3.81	4.08	3.82
F3U	4.17	4.12	3.81	4.08	3.83
L1U	3.04	3.24	3.43	3.23	3.46
L2U	3.22	3.30	3.47	3.29	3.50
L4U	3.27	3.36	3.54	3.35	3.58
R1U	3.20	3.21	3.46	3.27	3.42
R2U	3.26	3.27	3.53	3.33	3.45
R4U	3.32	3.33	3.61	3.40	3.52

NASA

National Aeronautical and  
Space Agency

# Report Document Page

1. Report No. 5-33173		2. Government Accession No.		3. Recipient's Catalog No.	
4. Title and Subtitle Shuttle PRCS Plume Contamination Analysis for Astro-2 Mission			5. Report Due April 30, 1993		
7. Author(s) Dr. F. C. Wang and C. Greene			8. Performing Organization Report No. 5-33173		
9. Performing Organization Name and Address UAH Research Institute University of Alabama in Huntsville Huntsville, AL 35899			10. Work Unit No. Purchase Order # P.O.H-18069D		
12. Sponsoring Agency Name and Address National Aeronautics and Space Administration George C. Marshall Space Flight Center Huntsville, Alabama 35812			11. Contract or Grant No. FNAS WANG MSFC PO		
			13. Type of report and Period covered Feb. 24, 1993 through April 30, 1993		
			14. Sponsoring Agency Code		
15. Supplementary Notes					
16. Abstract  <p>The Astro-2 mission scheduled for January 1995 flight is co-manifested with the Spartan experiment. The Astro instrument array consists of several telescopes operating in the UV spectrum. To obtain the desired 300 observations with the telescope array in a shorter time than the Astro-1 mission, it will be necessary to use the primary reaction control system (PRCS) rather than just the Vernier reaction control system. The high mass flow rate of the PRCS engines cause considerable concern about contamination due to PRCS plume return flux.</p> <p>Performance of these instruments depends heavily on the environment they encounter. The ability of the optical system to detect a remote signal depends not only on the intensity of the incoming signal, but also on the ensuing transmission loss through the optical train of the instrument. Performance of these instruments is thus dependent on the properties of the optical surface and the medium through which it propagates. The on-orbit contamination environment will have a strong influence on the performance of these instruments.</p> <p>This report summarizes the finding of a two-month study of the molecular contamination environment of the Astro-2 instruments due to PRCS thruster plumes during the planned Astro-2 mission.</p>					
17. Key Words (Suggested by Author(s)) PRCS Plumes Contamination Analysis Return Flux Column Densities Astro-2 Mission UV Telescope			18. Distribution Statement		
19. Security Class. (of this report) Unclassified		20. Security Class. (of this page) Unclassified		21. No. of pages	22. Price